Hepatic Changes Produced by a Single Dose of Endotoxin in the Mouse

Electron Microscopy

Emmanuel Levy,* M.D., Ph.D., F.C.Path.,
Ruby J. Slusser, and Boris H. Ruebner, M.D.

THE HEPATIC LESIONS observed in the mouse by light microscopic techniques, including histochemistry, following a single injection of endotoxin have been described previously.[1] Among the changes are a leukocytic reaction in the sinusoids, swelling of the Kupffer cells, platelet and fibrin thrombi, glycogen depletion, fatty metamorphosis, and changes in the location and intensity of the acid alkaline phosphatase reactions. There have been few studies by electron microscopy of the effects of a single injection of endotoxin, and these have concentrated on intravascular events.[2,3] An electron microscopic study of the mouse liver following injection of endotoxin was therefore undertaken in an attempt to clarify the resulting cellular events and to provide an ultrastructural basis for some of the known biochemical changes.

Materials and Methods

Pathogen-free CD_1 mice, 6–8 weeks old (Charles River Laboratories) were used. They were maintained for 2 days on Purina Pur Pak Lab Chow (pathogen free) with water ad libitum; food was withheld starting the evening before injection.

The endotoxin was Difco Bacto Lipopolysaccharide *E. coli* 0111:B4, prepared by a modification of the Boivin technique and suspended in sterile pyrogen-free water (Cutter Laboratories, Berkeley, Calif. so that 100 μg. or 300 μg. were contained in 0.1 ml. A total of 44 animals received intravenous injections in the tail vein, as previously reported.[1] Control animals were given 0.1 ml. of the sterile pyrogen-free water.

Samples of liver for electron microscopy were taken from 12 animals—3 after ½ hr., 3 after 1 hr., 3 after 4 hr., and 3 after 24 hr. In addition, material from 6 control animals was examined. The tissue was fixed in osmic acid[4] and embedded in Araldite. Sections 1 μ thick were cut on a Porter Blum MT-1 microtome and stained with toluidine blue for preliminary screening. Thin sections were cut on a Porter Blum MT-2 microtome, mounted on bare 400-mesh copper grids, and stained with lead

From the Department of Pathology, The Johns Hopkins University School of Medicine, Baltimore, Md.

Supported by Research Grants AI03958 and 5-RO1-AM-00660-13 and by a Research Career Development Award (Dr. Ruebner) from the National Institutes of Health, U.S. Public Health Service, by the Commonwealth Fund (Dr. Levy), and by Contract No. DA-49-193-MD-2310, Office of the Surgeon General, Department of the Army.

Accepted for publication Oct. 31, 1967.

Address for reprint requests: Dr. Ruebner, Department of Pathology, Johns Hopkins University School of Medicine, Baltimore, Md.

* Present address: Pathology Department, Central Emek Hospital, Affula, Israel.

citrate[5] or uranyl acetate or both. Sections were examined with an RCA EMU 3G or 3H electron microscope.

Results

The general ultrastructure of the liver is well known,[6,7] and several studies have dealt with particular aspects of the mouse liver.[8–17] The findings in the control animals agreed with these observations and will not be described unless they appear necessary to elucidate the changes in animals given endotoxin injections.

The changes observed at various times after endotoxin injection were focal and varied somewhat in different animals. The predominant changes at any particular sampling interval will be described.

Half-Hour Specimens

Hepatocytes. Occasional mitochondria showed slight swelling. The vesicles of the Golgi zones were filled with homogeneous, moderately electron-dense material resembling that found in controls, but were larger and often more numerous. In addition the vesicles contained electron-opaque particles of variable shape and density measuring 450–900 Å (Fig. 1). Some of the particles showed increased density at their periphery. There was moderate dilatation of the endoplasmic reticulum (ER) and some degranulation of the rough ER. Some of the dilated ER vesicles contained opaque particles which resembled those in the Golgi zones but were somewhat smaller (150–225 A), and other ER vesicles contained only homogeneous material. Glycogen granules appeared reduced compared with those found in controls.

Spherical or oval vacuoles measuring from 1.6 μ to 5 μ in diameter, never seen in controls, were quite prominent. They had a single limiting membrane, were generally situated between the nucleus and the sinusoidal border, and were usually at some distance from the cell membrane. These vacuoles contained material which was less electron-dense than that in the mitochondria and was finely granular at high magnification. Occasionally the vacuoles also contained strands of electron-dense material measuring from 0.5 μ to 1.5 μ in length and 70 mμ to 140 mμ in width with a periodicity of approximately 150 A, which corresponds to the periodicity of fibrin in the mouse.[18] In addition some roughly spherical vesicles with double membranes, which may have originated from the ER, were present (Fig. 2), and scattered granules varying from 500 to 750 Å in diameter, resembling those in the Golgi zones, were also visible. Dense bodies, resembling those shown by electron histochemistry to contain high acid phosphatase activity[8] and therefore thought to be lysosomes, were often seen in contact with the outer surface of the vacuoles.

Aggregates of granules, resembling those composing dense bodies but without limiting membranes, were sometimes seen within the vacuoles adjacent to the lining membrane (Fig. 3). In addition there were fairly numerous, strongly electron-dense particles approximately 50 Å in diameter which at high power consisted of 2–4 subunits arranged in a manner typical of ferritin.[19] A second type of vacuole not seen in the hepatocytes of control animals was also observed. These were round to oval with a diameter varying from 0.6 μ to 1.1 μ. Their contents were similar in density to that of mitochondria and appeared amorphous at low magnification and finely granular at higher magnification. Embedded in this material were small, dense granules compatible with ferritin, as well as occasional larger granules similar to those described in the Golgi apparatus but somewhat paler. In these vacuoles there were occasional vesicles lined by single membranes.

The dense bodies generally maintained their normal pericanalicular distribution. Most of them were composed of intensely electron-opaque particles. Occasionally one of the dense bodies was swollen along part of its periphery, with separation of the membrane from the core. Cytosegresomes were occasionally seen, usually containing incorporated mitochondria. Microbodies and multivesicular bodies, particularly in the neighborhood of the Golgi apparatus and near the sinusoidal border, appeared to be increased in number although they were not studied quantitatively (Fig. 4). The zone of the hepatocytes adjoining the sinusoid often showed marked swelling extending into the microvilli (Fig. 5). At high magnification, ferritin particles scattered through the cytoplasm were prominent. The perisinusoidal zone often showed prominent vesicles which contained material similar to that in the ER and Golgi apparatus. The nucleus showed focal moderate dilatations of the perinuclear space, within which occasional moderately dense particles were seen, similar to those described in the ER. The nuclear pores were prominent and in some areas apparent breaks were seen with the extrusion of granular material into the surrounding cytoplasm. Occasional bile canaliculi were dilated and had lost some of their microvilli.

The space of Disse appeared moderately dilated and contained prominent dense particles, 300–1200 Å in diameter, resembling those in the Golgi and the ER. Usually the particles were located between microvilli without being actually attached to them (Fig. 6). The swollen microvilli were often embedded in "fuzzy" electron-dense material without any periodicity; similar material was much less abundant in control animals.

Sinusoids. The Kupffer cells showed moderate cytoplasmic swelling, with occasional myelin figures present within the cytosomes. Some of the

mitochondria had an increased number of cristae, which occasionally lost the normal perpendicular orientation to the outer membranes. Focal dilatation of the space between the outer and inner membranes, resembling that in the hepatocytes, was sometimes seen. In a few places there were discontinuities of the cell membrane, suggesting increased fragility and subsequent rupture, possibly during processing. In the cytoplasm there were some vacuoles similar to the smaller type described in the hepatocytes; these were seen infrequently in control animals.

Platelets were common, often in groups of 5 or 6. These were often arranged in a mosaic pattern (Fig. 7). Individual platelets showed deformation with loss of their normal round or oval shape and pseudopodia. Surrounding these aggregates and between individual platelets there was electron-dense fuzzy material similar to that surrounding swollen microvilli in the space of Disse. Although the majority of the platelets retained several specific granules in their central areas, the periphery often appeared swollen and degranulated. Some of the granules showed varying degrees of vacuolation and rarely contained material with a periodicity of 160 Å corresponding to fibrin. Scattered particles of 2 main types were also found; the smallest and most electron-dense particles measured up to 100 Å in diameter and were similar to ferritin, while the second type measured approximately 250 Å, and was probably glycogen.

Lymphocytes, eosinophils, and neutrophils were occasionally encountered; these showed no special features except that the neutrophils contained granules measuring 250 Å, which were similar to those seen in the platelets and were most probably glycogen. The specific granules of the leukocytes showed some vacuolation.

The swollen microvilli of the hepatocytes and their surrounding coat of electron-dense material, together with the swollen Kupffer cells and platelets were sufficient in many places to fill the sinusoidal space.

One-Hour Specimens

Hepatocytes. The mitochondrial swelling increased, with some of the cristae tending to loop at the periphery instead of extending into the organelle. Occasional mitochondria showed a marked loss of cristae. The prominence of the Golgi apparatus was greater than at the half-hour interval, and the contents of the vesicles were either uniformly or moderately electron-dense, or showed scattered, dense particles, mainly peripheral, on a less dense background. The amount of glycogen was markedly reduced. The ER, particularly in the perisinusoidal zones, showed more dilatation than at half an hour, and many vesicles contained from 1 to 3 particles similar to those in the Golgi apparatus. The large vacuoles were reduced in number and size compared with the half-hour specimens. The

lysosomes showed 2 apparent changes; those with closely-packed, strongly electron-dense particles were reduced in number while those showing fewer and less dense granules were increased; their location appeared to be less definitely pericanalicular. The perisinusoidal zone showed a persistent increase in microbodies and multivesicular bodies with swollen microvilli. Vesicles, many of which contained particles similar to those noted in the space of Disse at half an hour, continued to be prominent (Fig. 8). Dilatation of bile canaliculi persisted.

The space of Disse now showed marked dilatation. Free particles were still conspicuous but perhaps somewhat fewer than in the half-hour specimens. The "fuzzy" material surrounding the microvilli had increased in prominence (Fig. 9).

Sinusoids. The swelling of the Kupffer cells increased. They showed some large vacuoles containing granular material of the type described in the hepatocytes at the half-hour interval. The ER, particularly the rough ER, appeared dilated and empty, sometimes markedly so (Fig. 10). The lysosomes seemed more numerous and swollen, with some apparent discharge of granules into the surrounding cytoplasm. Some cytosegresomes were also seen. Areas of necrosis of the hyaline body type [20,21] were occasionally seen (Fig. 11). The focal dilatation of the perinuclear space continued to be prominent with occasional rupture of membranes and extrusion of granular material (Fig. 12). Smaller vacuoles of the type described at the half-hour interval appeared more numerous (Fig. 13).

Four-Hour Specimens

Hepatocytes. Focal swelling of the hyaloplasm and swelling of mitochondria became more pronounced than previously. The number of lysosomes appeared to be decreased in the pericanalicular zones and more prominent in the perinuclear area; many showed varying degrees of vacuolation (Fig. 14). Golgi vesicles remained prominent, both near the nuclei and in the pericanalicular zones. The ER continued to show dilatation, now somewhat less marked. Occasional vacuoles varying from 0.7 μ to 1.0 μ in diameter could still be seen, now usually located near the sinusoidal border. Some smaller vacuoles with granular contents were present. Microbodies continued to be prominent. The swelling of the sinusoidal microvilli and the surrounding electron-dense material persisted. Bile canaliculi continued to be dilated.

The space of Disse continued to be widened but there seemed to be a reduction in the number of 500–750 Å particles. Free mitochondria and glycogen particles were occasionally seen (Fig. 9). Platelet aggregations and neutrophils persisted in the sinusoids.

The Kupffer cells continued to be swollen with dilated ER and showed

a persistent increase in lysosomes. Cytosegresomes containing membrane structures, particularly mitochondria, and foci of necrosis were seen (Fig. 15). Vacuoles were more numerous than in samples taken at earlier intervals. Focal perinuclear dilatation persisted.

Twenty-four-Hour Specimens

Hepatocytes. Striking swelling of the mitochondria with marked peripheral looping of cristae was seen, along with some continued dilatation of the ER and persistence of dilated Golgi vesicles. In some areas there was reconstitution of the rough ER. Lysosomes continued to show vacuolation. Foci of necrosis were now present (Fig. 16). The number of large lipid droplets was increased.

In the space of Disse platelets embedded in fuzzy material persisted. The sinusoidal microvilli appeared to be increased. Bile canaliculi showed persistence of dilatation and reduction in the microvilli (Fig. 17).

Discussion

The dose of endotoxin employed in this investigation has a high mortality in conventional mice but was found by previous workers [22] and in our investigations [1] to have no lethal effects on pathogen-free animals.

The particles in the space of Disse, ER, and Golgi vesicles appeared to be identical. A smaller number of similar particles in these sites has been described in normal mice [12,16] and rats.[23–25] Our controls showed occasional particles in the Golgi apparatus and ER but not in the space of Disse. An increase in these particles resembling that described here has been observed after ethanol [26] or carbon tetrachloride,[27] choline deficiency,[28] liver regeneration,[29] administration of adenine to ethionine-treated rats,[30] and fatty acid infusion.[25,31,32] These particles were considered to be albumin,[23] lipid, or lipoprotein.[25,26,29–31] The size range of our particles is within that for lipoprotein (100–1000 Å),[33,34] and it seems likely that they consist of low-density lipoprotein.[25] These findings could be the result of stimulation of the adrenal cortex by endotoxin,[35] which leads to mobilization of fatty acids from the body stores,[36] and increased synthesis and excretion of lipoprotein by hepatocytes.[25,31,32] It seems unlikely that any of the other alterations we observed, except possibly some of the mitochondrial swelling, could have been the result of steroid stress.[34] Another possible explanation for the increased number of lipoprotein particles could be liberation of hepatic fatty acids by the endotoxin.[38] The decreased number of these particles after the first hour following injection of endotoxin may be due to interference with protein synthesis. This suggestion would be consistent with the changes which we observed in the ER.

Vacuoles are produced in the parenchymal cells of the liver by hypoxia,[39-41] chemical hepatotoxins,[42,43] hypertonic solutions,[44,45] dietary deficiences,[40,46] alloxan,[47] and partial hepatectomy.[48] The large vacuoles which we observed resembled hypoxic vacuoles in their size, the speed of their development, and their association with congestion and reduction in glycogen. Reduction of hepatic oxygen tension after doses of endotoxin has been reported[49] and may have been caused by swelling of Kupffer cells and hepatocytes, vascular occlusion by platelet thrombi, and aggregates of circulating cells and congestion.[1,50,52] The comparatively small number of vacuoles would suggest that hypoxia was only moderate. Hypoxic vacuoles appear empty or contain only proteinaceous material[41,44,53,54] while our vacuoles contained granular and membranous material and resembled the vacuoles induced by dextran[8] and sucrose,[45] in which lysosomes are thought to be concerned. Factors other than anoxia—such as intake of endotoxin in colloidal suspension—probably contributed, therefore, to the formation of the large vacuoles. The fibrin in these vacuoles also suggests the presence of endotoxin since endotoxin can produce fibrin from plasma proteins[55] which the vacuoles are known to contain.[56] Although fibrin with characteristic periodicity was not observed in the sinusoids, entry of fibrin into the vacuoles by phagocytosis remains possible. The origin of the large vacuoles from a particular organelle[43,57] has not been established, perhaps because the first specimens were not taken until half an hour after injection and vacuoles may form within a few minutes.[40,42,58] The smaller hepatocytic vacuoles probably represent swollen lysosomes or cytosegresomes, an interpretation in keeping with their subsequent appearance in Kupffer cells. Since dextran apparently does not cause ultrastructural changes other than vacuole formation,[8] the other morphologic changes described here probably represent toxic effects of endotoxin.

The decreased alkaline phosphatase activity of the bile canaliculi with increased sinusoidal activity reported by light microscopy[1] may be correlated with the decreased number of canalicular microvilli that we observed. The possibility of metabolic disturbances at these sites in association with the development of vacuoles has been suggested in previous reports.[40,44,58] The changes in the lysosomes correlate to some extent with our previous histochemical observations.[1] The reduced acid phosphatase activity noted at 24 hr. by light microscopy would seem to parallel the reduction in pericanalicular lysosomes observed by electron microscopy and their replacement by electron-light lysosomes of the Type II of Daems and van Rijssel.[11] The decreased density of the lysosomes might be the result of the release of enzymes including acid phosphatase as determined by biochemical methods.[53-61] No definite basis, at the ultra-

structural level, has been found for the increase in acid phosphatase demonstrated by light microscopy at 4 hr. Although the dense lysosomes appeared prominent, it was not possible to assess them quantitatively. However, the change in location of the lysosomes seen by electron microscopy is in keeping with the light microscopic observation of acid phosphatase activity in the perinuclear zone.[1] The increased number of lysosomes in the Kupffer cells correlates well with the marked acid phosphatase activity observed by light microscopy. The mitochondrial swelling and vacuolation of the ER could correlate respectively with the reduction in succinic dehydrogenase and glucose-6-phosphatase activity suspected by light microscopy.[1]

The platelet thrombi which we observed electron microscopically correspond to our light microscopic observations.[1] Morphologically the platelets composing the thrombi showed the features of thrombosis before the onset of viscous metamorphosis.[62–64] The material found occasionally within platelets with a periodicity like that of fibrin is probably normal.[18]

There are at least 3 possible interpretations for the electron-dense material which we observed in the sinusoids and between the platelets. "Fuzz" between the microvilli of normal animals has been regarded as equivalent to a basement membrane by some,[12,67,69] while others deny the existence of such a membrane under normal circumstances.[10,70,71] In our controls, fuzz was observed in the space of Disse and may have represented fragments of basement membrane, plasma protein, or secretory material.[31,68] In our experimental animals this material in the space of Disse was increased and resembled basement membrane more closely, as has been reported previously in hypoxia,[42] viral hepatitis,[72–74] cirrhosis,[75,76] and acute experimental trauma.[69] While some of the "fuzziness" around the platelets may have been the result of tangential membrane sectioning, the material seen, particularly in this location, may well have represented fibrin not polymerized sufficiently to develop a characteristic axial periodicity. Electron microscopically, fibrin is usually fibrillar and only rarely shows axial periodicity.[2,64–66] Another possible source for the electron-dense material in the space of Disse is phospholipid release from platelets, which may occur in coagulation.[77–79] A single dose of endotoxin produced fibrin without platelet thrombi in rabbits[2] while pregnant rats developed a Shwartzman-like phenomenon and showed platelet thrombi with fibrin.[3] The relative insusceptibility of mice to the Shwartzman reaction may be correlated with the relatively small amount of fibrin-like material which we found in the sinusoids.

In view of the changes in the sinusoids, bile canaliculi, and cell organelles as well as the cytochemical changes,[1] it is suggested that endo-

toxin may act primarily on membranes. However, this could be proved only by localizing the endotoxin Since endotoxin preparations are colloidal suspensions, it should be possible to visualize the particles by electron microscopy. Negative staining of an endotoxin preparation revealed particles of 240–1400 Å,[80] and shadow casting of endotoxin hydrolysates demonstrated particles with a wide range of morphologic appearances.[81] Although we were unable to identify endotoxin particles, we believe that the pinocytotic vesicles at the sinusoidal border of the hepatocyte in the early stage of the present experiment may be associated with intake of endotoxin. More refined methods for identifying and labeling endotoxin at the ultrastructural level should elucidate its site and mechanism of action.

Summary

The effects on the mouse liver of a single injection of endotoxin have been studied by electron microscopy.

Hepatocytes showed vacuolation, dilatation of endoplasmic reticulum, and mitochondrial swelling, with lysosomal changes and increase in microbodies and multivesicular bodies; the amount of cell glycogen was decreased and lipid increased. Increased lipoprotein production was suggested by the appearance of electron-dense particles in the endoplasmic reticulum, Golgi apparatus, and the space of Disse. Areas of necrosis were also found.

Kupffer cells showed early swelling and membrane damage, with increased numbers of lysosomes and vacuoles. Possible damage to the nuclear membrane was also seen as well as acidophilic bodies and areas of necrosis.

The space of Disse was widened and contained increased electron-dense material. The sinusoids showed platelet thrombi and circulating cells including lymphocytes, neutrophils, and eosinophils.

The bile canaliculi were dilated.

These findings have been correlated with previous light microscopic observations, and their pathogenesis has been discussed. The need for more accurate localization of the site of endotoxin has been stressed.

References

1. Levy, E., and Ruebner, B. H. Hepatic changes produced by a single dose of endotoxin in the mouse: light microscopy and histochemistry. *Amer J Path* 51:269–285, 1967.
2. Prose, P. H., Lee, L., and Balk, S. D. Electron microscopic study of the phagocytic fibrin-clearing mechanism. *Amer J Path* 47:403–417, 1965.

3. McKay, D. G., Margaretten, W., and Csavossy, I. An electron microscope study of the effects of bacterial endotoxin on the blood vascular system. *Lab Invest 15*:1815–1829, 1966.
4. Millonig, G. "Further Observations on a Phosphate Buffer for Osmium Solutions in Fixation." In *Electron Microscopy*, Breese, S. S., Jr., Ed. Acad. Press, New York, 1962, p. 8.
5. Venable, J. H., and Coggeshall, R. A simplified lead citrate stain for use in electron microscopy. *J Cell Biol 25*:407–408, 1965.
6. Rouiller, C., Ed. *The Liver. Morphology, Biochemistry, Physiology* (Vol. I.). Acad. Press, New York, 1963.
7. David, H. *Submicroscopic Ortho-and Pathomorphology of the Liver*. Macmillan, New York, 1964.
8. DeMan, J. C. H., Daems, W. T., Willighagen, R. G. J., and van Rijssel, T. G. Electron-dense bodies in liver tissue of the mouse in relation to the activity of acid phosphatase. *J Ultrastruct Res 4*:43–57, 1960.
9. Schmidt, F. C. Elektronenmikroskopische Untersuchungen an den Sinuswandzellen (Kupfferschen Sternzellen) der weissen Maus. *Anat Anz 108*: 376–387, 1960.
10. Daems, W. T. The micro-anatomy of the smallest biliary pathways in mouse liver tissue. *Acta Anat (Basel) 46*:1–24, 1961.
11. Daems, W. T., and van Rijssel, T. G. The fine structure of the peri-biliary dense bodies in mouse liver tissue. *J Ultrastruct Res 5*:263–290, 1961.
12. Trump, B. F., Goldblatt, P. J., and Stowell, R. E. An electron microscopic study of early cytoplasmic alterations in hepatic parenchymal cells of mouse liver during necrosis in vitro (autolysis). *Lab Invest 11*:986–1015, 1962.
13. Trump, B. F., Goldblatt, P. J., and Stowell, R. E. Studies on necrosis of mouse liver in vitro. Ultrastructural alterations in the mitochondria of hepatic parenchymal cells. *Lab Invest 14*:343–371, 1965.
14. Trump, B. F., Goldblatt, P. J., and Stowell, R. E. Studies of necrosis in vitro of mouse hepatic parenchymal cells. Ultrastructural and cytochemical alterations of cytosomes, cytosegresomes, multivesicular bodies, and microbodies and their relation to the lysosome concept. *Lab Invest 14*:1946–1968, 1965.
15. Trump, B. F., Goldblatt, P. J., and Stowell, R. E. Studies of mouse liver necrosis in vitro. Ultrastructural and cytochemical alterations in hepatic parenchymal cell nuclei. *Lab Invest 14*:1969–1999, 1965.
16. Trump, B. F., Goldblatt, P. J., and Stowell, R. E. Studies of necrosis in vitro of mouse hepatic parenchymal cells. Ultrastructural alterations in endoplasmic reticulum, Golgi apparatus, plasma membrane and lipid droplets. *Lab Invest 14*:2000–2028, 1965.
17. Shnitka, T. K. Comparative ultrastructure of hepatic microbodies in some mammals and birds in relation to species differences in uricase activity. *J Ultrastruct Res 16*:598–625, 1966.
18. Martin, M. Über Fibrinähnliche Einschlusse in Thrombozyten der Maus. Eine Elektronenmikroskopische Studie. *Z Zellforsch 76*:108–115, 1967.
19. Kuff, E. L., and Dalton, A. J. Identification of molecular ferritin in homogenates and sections of rat liver. *J. Ultrastruct Res 1*:62–73, 1957.
20. Biava, C., and Mukhlova-Montiel, M. Electron microscopic observations on Councilman-like acidophilic bodies and other forms of acidophilic changes in human liver cells. *Amer J Path 46*:775–802, 1965.

21. KLION, F. M., and SCHAFFNER, F. The ultrastructure of acidophilic "Councilman-like" bodies in the liver. *Amer J Path 48*:755–767, 1966.

22. SCHAEDLER, R. W., and DUBOS, R. J. The fecal flora of various strains of mice. Its bearing on their susceptibility to endotoxin. *J Exp Med 115*:1149–1160, 1962.

23. BRUNI, C., and PORTER, K. R. The fine structure of the parenchymal cell of the normal rat liver. I. General observations. *Amer J Path 46*:691–755, 1965.

24. GLINSMANN, W. H., and ERICSSON, J. L. E. Observations on the subcellular organization of hepatic parenchymal cells. II. Evolution of reversible alterations induced by hypoxia. *Lab Invest 15*:762–777, 1966.

25. JONES, A. L., RUDERMAN, N. B., and HERRERA, M. G. An electron microscope study of lipoprotein production and release by the isolated perfused rat liver. *Proc Soc Exp Biol Med 123*:4–9, 1966.

26. STEIN, O., and STEIN, Y. Fine structure of the ethanol induced fatty liver in the rat. *Israel J Med Sci 1*:378–388, 1965.

27. REYNOLDS, E. S. Liver parenchymal cell injury. I. Initial alterations of the cell following poisoning with carbon tetrachloride. *J Cell Biol 19*:139–157, 1963.

28. ASHWORTH, C. T., SAUNDERS, E., and ARNOLD, N. Hepatic lipids: Fine structural changes in liver cells after high fat, high cholesterol, and choline deficient diet in rats. *Arch Path (Chicago) 72*:625–636, 1961.

29. TROTTER, N. L. A fine structure study of lipid in mouse liver regenerating after partial hepatectomy. *J Cell Biol 21*:233–244, 1964.

30. LOMBARDI, B. Considerations on the pathogenesis of fatty liver. *Lab Invest 15*:1–20, 1966.

31. HAMILTON, R. L., REGEN, D. M., GRAY, M. E., and LEQUIRE, V. S. Lipid transport in liver. 1. Electron microscopic identification of very low density lipoproteins in perfused rat liver. *Lab Invest 16*:305–319, 1967.

32. STEIN, O., and STEIN, Y. Lipid synthesis, intracellular transport, storage and secretion. 1. Electron microscopic radioautographic study of liver after injection of tritiated palmitate or glycerol in fasted and ethanol-treated rats. *J Cell Biol 33*:319–339, 1967.

33. HAYES, T. L., and HEWITT, J. E. Visualization of individual lipoprotein macromolecules in the electron microscope. *J Appl Physiol 11*:425–428, 1957.

34. CASLEY-SMITH, J. R. The identification of chylomicra and lipo-proteins in tissue sections and their passage into jejunal lacteals. *J Cell Biol 15*:259–277, 1962.

35. EGDAHL, R. H. The differential response of the adrenal cortex and medulla to bacterial endotoxin. *J Clin Invest 38*:1120–1125, 1959.

36. HILL, R. B., DROKE, W. E., and HAYS, A. P. Hepatic lipid metabolism in the cortisone-treated rat. *Exp Molec Path 4*:320–327, 1965.

37. RUEBNER, B. H., HIRANO, T., and SLUSSER, R. J. Electron microscopy of the hepatocellular and Kupffer cell lesions of mouse hepatitis with particular reference to the effect of cortisone. *Amer J Path 51*:163–189, 1967.

38. FARRAR, W. E., and CORWIN, L. M. The essential role of the liver in detoxification of endotoxin. *Ann NY Acad Sci 133*:668–684, 1966.

39. TROWELL, O. A. The experimental production of watery vacuolation of the liver. *J Physiol (London) 105*:268–297, 1946.

40. GILLMAN, J., and GILLMAN, T. Anoxia and the liver with special reference to shock and chronic malnutrition. *S Afr J Med Sci 13*:11–43, 1948.

41. MÖLBERT, E., and GUERRITORE, D. Elektronenmikroskopische Untersuchungen an Leberparenchym bei akuter Hypoxie. *Beith Path Anat 117*:32–49, 1957.

42. MÖLBERT, E. Das Elektronenmikroskopische Bild der Leberparenchymzelle nach histotoxischer Hypoxydose. *Beitr Path Anat 118*:203–227, 1957.

43. ASHWORTH, C. T., WERNER, D. J., GLASS, M. D., and ARNOLD, N. J. Spectrum of fine structural changes in hepatocellular injury due to thioacetamide. *Amer J Path 47*:917–951, 1965.

44. ATERMAN, K. Observations on the nature of "watery vacuolation". The response of the liver cell to the intravenous injection of hypertonic saline, Evans blue, dextran and heparin. *Lab Invest 7*:577–605, 1958.

45. BREWER, D. B., and HEATH, D. Development of sucrose vacuoles from liver cell lysosomes. *J Path Bact 87*:405–408, 1964.

46. ELAM, R., and HEIFETZ, C. J. Experimental hypoalbuminemia. Its effect on the morphology, function, and protein and water content of the liver. *J Exp Med 73*:417–430, 1941.

47. DUBOIS, A. M. Actions de l'intoxication alloxanique sur le foie de cobaye. Z *Zellforsch 40*:585–604, 1954.

48. DONIACH, I., and WEINBREN, K. The development of inclusion bodies in the cells of the rat's liver after partial hepatectomy. *Brit J Exp Path 33*:499–505, 1952.

49. MATSUZAWA, T., and WILSON, R. Oxygen changes in tissues of germ free and conventional mice after inoculation of bacterial endotoxin. *Tohoku J Exp Med 85*:361–364, 1965.

50. GILBERT, R. Mechanisms of the hemodynamic effects of endotoxin. *Physiol Rev 40*:245–279, 1960.

51. ZWEIFACH, B. W. "Vascular Effects of Bacterial Endotoxin." In *Bacterial Endotoxins*, LANDY, M., and BRAUN, W., EDS. Quinn and Boden, Rahway, N. J., 1964, pp. 110–117.

52. NOLAN, J. P. and O'CONNEL, J. Vascular response in isolated rat liver. I. endotoxin, direct effects. *J Exp Med 122*:1063–1073, 1965.

53. OUDEA, P. R. Anoxic changes of liver cells. Electron microscopic study after injection of colloidal mercury. *Lab Invest 12*:386–394, 1963.

54. HANZON, V. Hypoxic vacuolization of the liver cell. *Proc Europ Conf Electron Microscopy (Delft) 2*:903–906, 1960.

55. MCKAY, D. G. *Disseminated Intravascular Coagulation. An Intermediary of Disease*. Hoeber, New York, 1965, pp. 212–243.

56. NAIRN, R. C., CHADWICK, C. S., and MCENTEGART, M. G. Fluorescent protein tracers in the study of experimental liver damage. *J Path Bact 76*:143–153, 1958.

57. STEINER, J. W., PHILLIPS, M. J., and BAGLIO, C. M. Electron microscopy of the excretory pathways in the liver in alpha-naphthyl isothiocyanate intoxication. A study of intrahepatic cholestasis. *Amer J Path 43*:677–696, 1963.

58. HANZON, V. Liver cell secretion under normal and pathologic conditions studied by fluorescence microscopy of living rats. VIII. O_2 deficiency and uranin secretion. *Acta Physiol Scand 28* (Suppl. 101):196–220, 1952.

59. JANOFF, A., and KALEY, G. "Studies on Lysosomes in Tolerance, Shock and Local Injury Induced by Endotoxin." In *Bacterial Endotoxins*, LANDY, M., and BRAUN, W., EDS. Quinn and Boden, Rahway, N. J., 1964, pp. 631–647.

60. WEISSMANN, G., and THOMAS, L. "On a Mechanism of Tissue Damage by Bacterial Endotoxins." In *Bacterial Endotoxins*, LANDY, M., and BRAUN, W., EDS. Quinn and Boden, Rahway, N. J., 1964, pp. 602–609.

61. GUTH, P. S., AMARO, J., SELLINGER, O. Z., and ELMER, L. Studies in vitro of the effects of chlorpromazine on rat liver lysosomes. *Biochem Pharmacol 14:* 769–775, 1965.

62. VASSALI, P., SIMON, G., and ROUILLER, C. Ultrastructural study of platelet changes initiated in vivo by thrombin. *J Ultrastruct Res 11*:374–387, 1964.

63. DAVID-FERREIRA, J. F. The blood platelet: electron microscopic studies. *Int Rev Cytol 17*:99–148, 1964.

64. STEHBENS, W. E., and BISCOE, T. J. The ultrastructure of early platelet aggregation in vito. *Amer J Path 50*:219–243, 1967.

65. STILL, W. J. S., and BOULT, E. H. Electron microscopic appearance of fibrin in thin sections. *Nature (London) 179*:868–869, 1957.

66. SHIRASAWA, K. Electron and light microscopic observations on experimental thrombosis. *Acta Path Jap 16*:1–36, 1966.

67. WASSERMAN, F. The structure of the wall of the hepatic sinusoids in the electron microscope. *Z Zellforsch 49*:13–32, 1958.

68. HAMPTON, J. C. A re-evaluation of the submicroscopic structure of the liver. *Texas Rep Biol Med 18*:602–611, 1960.

69. COSSEL, L. Über akutes Auftreten von Basalmembranen an den Lebersinusoiden. *Beitr Path Anat 134*:103–122, 1966.

70. BENNETT, S., LUFT, J. H., and HAMPTON, J. C. Morphological classifications of vertebrate blood capillaries. *Amer J Physiol 196*:381–390, 1959.

71. DAVID, H. Zur Morphologie der Leberzellmembran. *Z Zellforsch 55*:220–234, 1961.

72. COSSEL, L. Elektronenmikroskopische Untersuchungen an den Lebersinusoiden bei Virushepatitis. *Klin Wschr 37*:1263–1278, 1959.

73. HOLLE, G. Über elektronenmikroskopische Befunde an der Leber bei Virushepatitis und zur Frage des hepatozellulären Ikterus. *Deutsch Med Wschr 85:* 2089–2093, 1960.

74. SCHAFFNER, F. Intralobular changes in hepatocytes and the electron microscopic mesenchymal response in acute viral hepatitis. *Medicine (Baltimore) 45*:547–552, 1966.

75. SCHAFFNER, F., and POPPER, H. Capillarization of hepatic sinusoids in man. *Gastroenterology 44*:239–242, 1963.

76. STEINER, J. W., JEZEQUEL, A. M., PHILLIPS, M. J., MIYAI, K., and ARAKAWA, K. "Some Aspects of the Ultrastructural Pathology of the Liver." In *Progress in Liver Diseases* (Vol. II.), POPPER, H., and SCHAFFNER, F., Eds. Grune, New York, 1965, pp. 351–352.

77. DESPREZ, R. M., HOROWITZ, H. I., and HOOK, E. W. Effects of bacterial endotoxin on rabbit platelets. 1. Platelet aggregation and release of platelet factors in vitro. *J Exp Med 114*:857–874, 1961.

78. RODMAN, N. F., MASON, R. G., MCDEVITT, N. B., and BRINKHOUS, K. M. Morphological alterations of human blood platelets during early phases of clotting. Electron microscopic observations of thin sections. *Amer J Path 40*:271–284, 1962.

79. WHITE, J. G., and KRIVIT, W. The ultrastructural localization and release of platelet lipids. *Blood 27*:167–186, 1966.

80. BLADEN, H. A., and MERGEN-HAGEN, S. E. Ultrastructure of Veillonella and morphological correlation of an outer membrane with particles associated with endotoxic activity. *J Bact* 88:1482–1492, 1964.

81. BEER, H., and BRAUDE, A. I. A study of particle sizes, shapes and toxicities in a Boivin-type endotoxin preparation. *Ann NY Acad Sci* 133:450–475, 1966.

We wish to thank Miss Joanne Alsruhe and Leslie Gilday for their histologic technical assistance, and Mr. Michael Friedman for assistance with the photography.

Legends for Figures

All illustrations are from animals that received 300 μg. of endotoxin intravenously. Sections are stained with lead citrate unless otherwise stated. Figures 1–7 are specimens obtained at one-half hour.

Fig. 1. Golgi apparatus in hepatocyte showing increased size and number of vesicles (arrows) containing electron-dense material interpreted as lipoprotein. Dense body (L) and microbody (M) are seen. × 35,800.

Fig. 2. Vacuole in hepatocyte showing fibrin strands with periodicity of 160 Å (arrow), some membranes, and scattered granules of various sizes. × 20,500.

Fig. 3. Vacuole in hepatocyte showing granular aggregates suggestive of origin from dense bodies (arrows) along inner surface of vacuole. One vesicle continuous with vacuole appears to represent discharged dense body (L). Uranyl acetate. × 16,500.

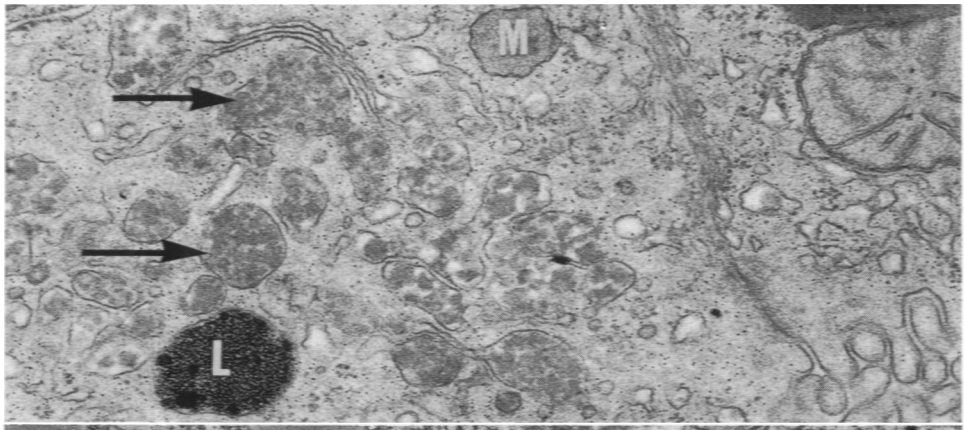

1

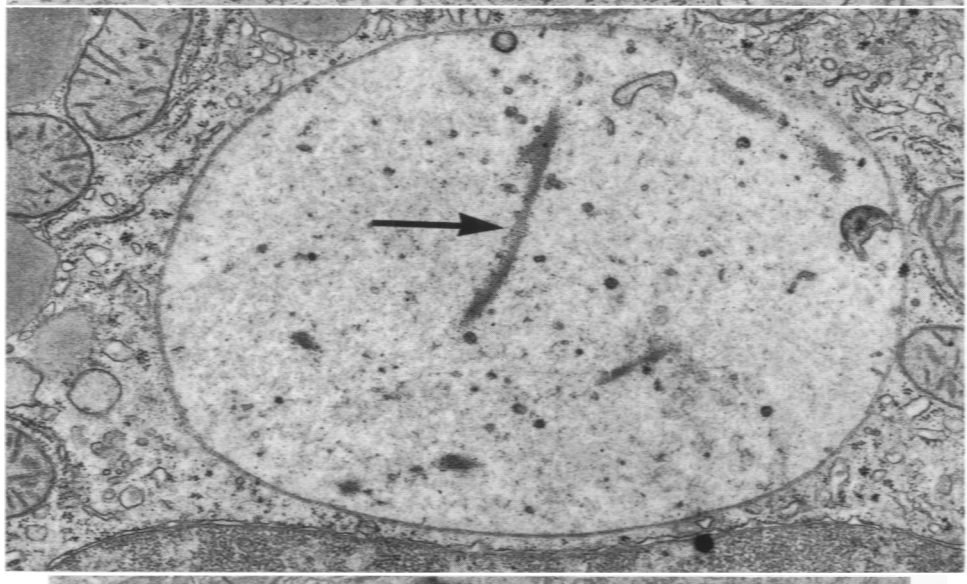

2

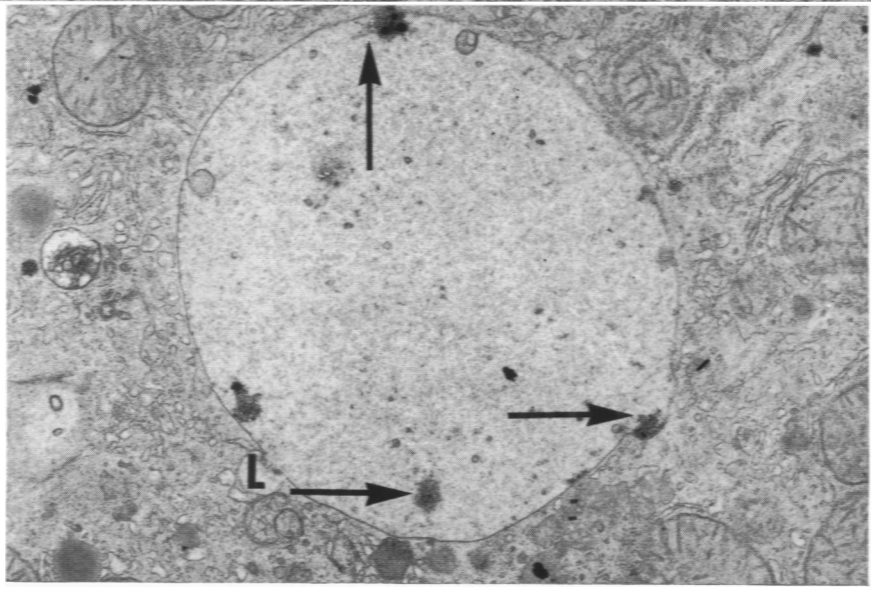

3

Fig. 4. Pericanalicular zone showing 2 cytosegresomes (arrows), prominent microbodies (M), and vacuolated dense bodies (L). × 16,000.

Fig. 5. Parasinusoidal zone of hepatocytes (H) showing marked swelling. Space of Disse shows prominent "fuzz" (F). Breaks in limiting membrane of swollen Kupffer cell visible (arrows). × 16,800.

Fig. 6. Lipoprotein particles (arrows) in space of Disse and dilated endoplasmic reticulum of hepatocytes. Surface membrane of Kupffer cell shows apparent breaks (barbed arrows). × 8800.

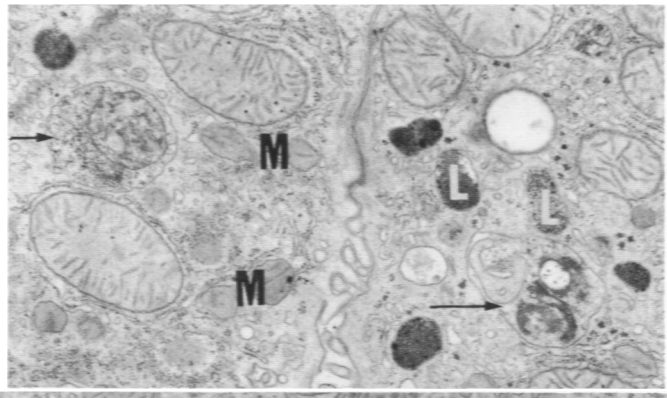

4

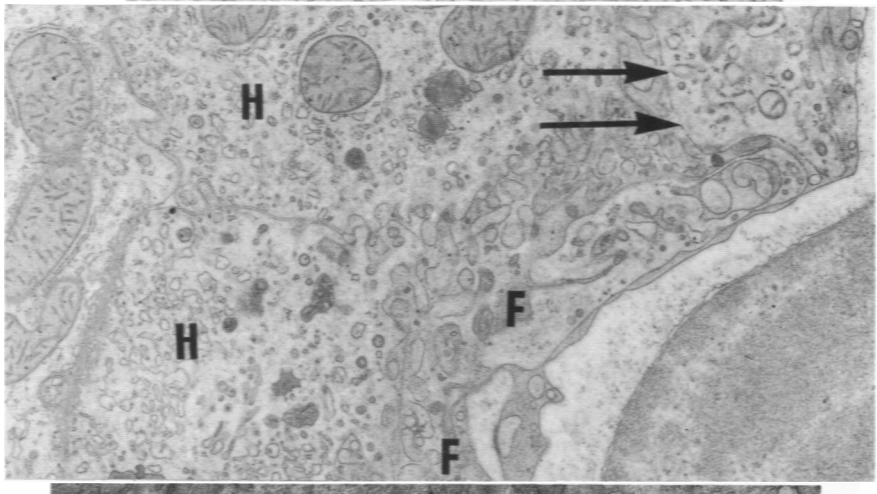

5

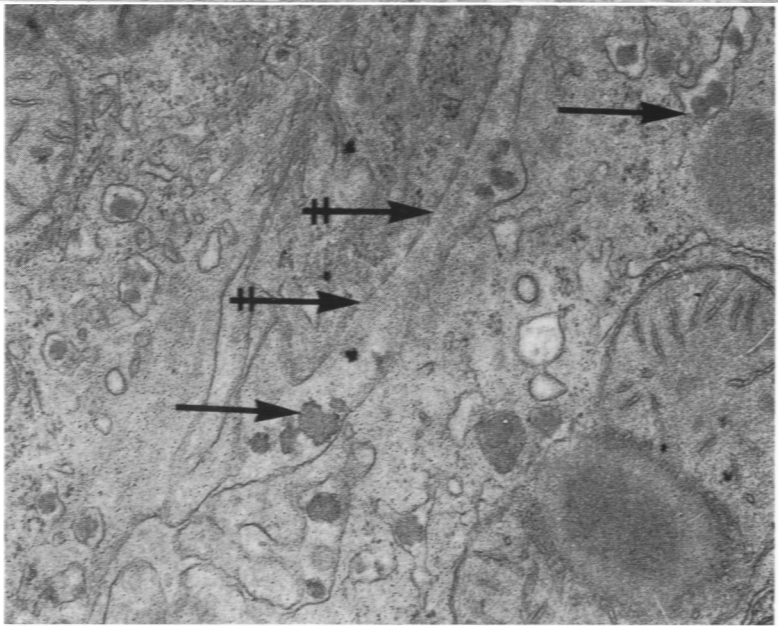

6

Fig. 7. Thrombus in sinusoid composed of platelets, some of which are degranulated and show pseudopodia (barbed arrows). Fuzzy material (arrow) is seen between platelets. × 10,000.

Fig. 8. At 1 hr. Prominent vesicles (arrows) along sinusoidal surfaces of hepatocytes. Some contain granular material (barbed arrows) suggesting reverse pinocytosis of lipoprotein particles. Empty vesicles may represent pinocytosis of unknown substances. × 20,600.

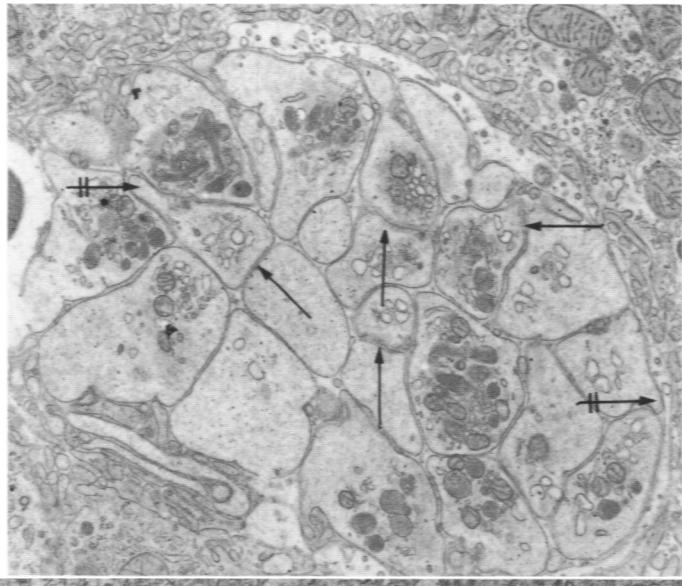

7

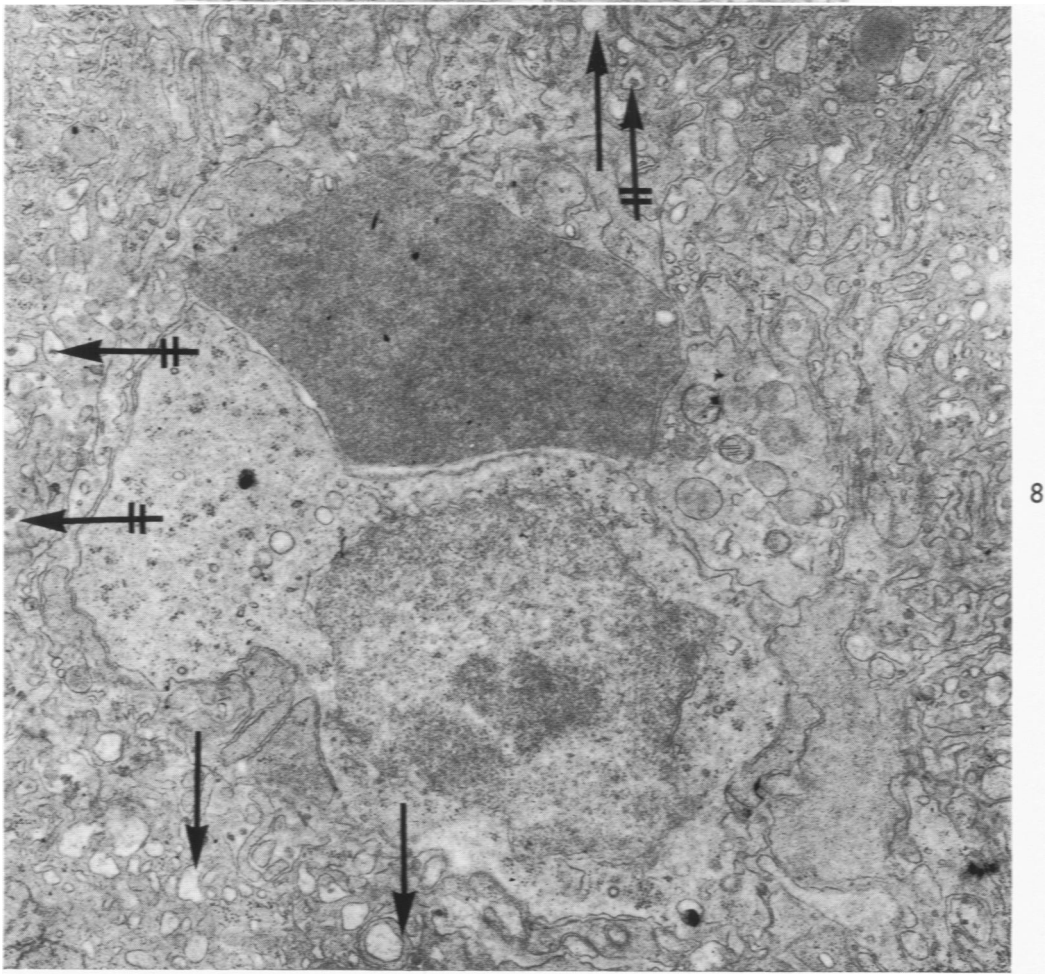

8

Fig. 9. At 4 hr. Increased electron-dense "fuzz" (arrows) surrounding microvilli. Some fibrillar material (F) is also seen. Space of Disse (D) enlarged, and contains free mitochondria and glycogen. Edge of hepatocytes (H) seen. K, Kupffer cell. × 20,100.

Fig. 10. At 1 hr. Marked dilatation of rough endoplasmic reticulum in Kupffer cell. Note separation of outer from inner nuclear membrane (arrows). × 30,300.

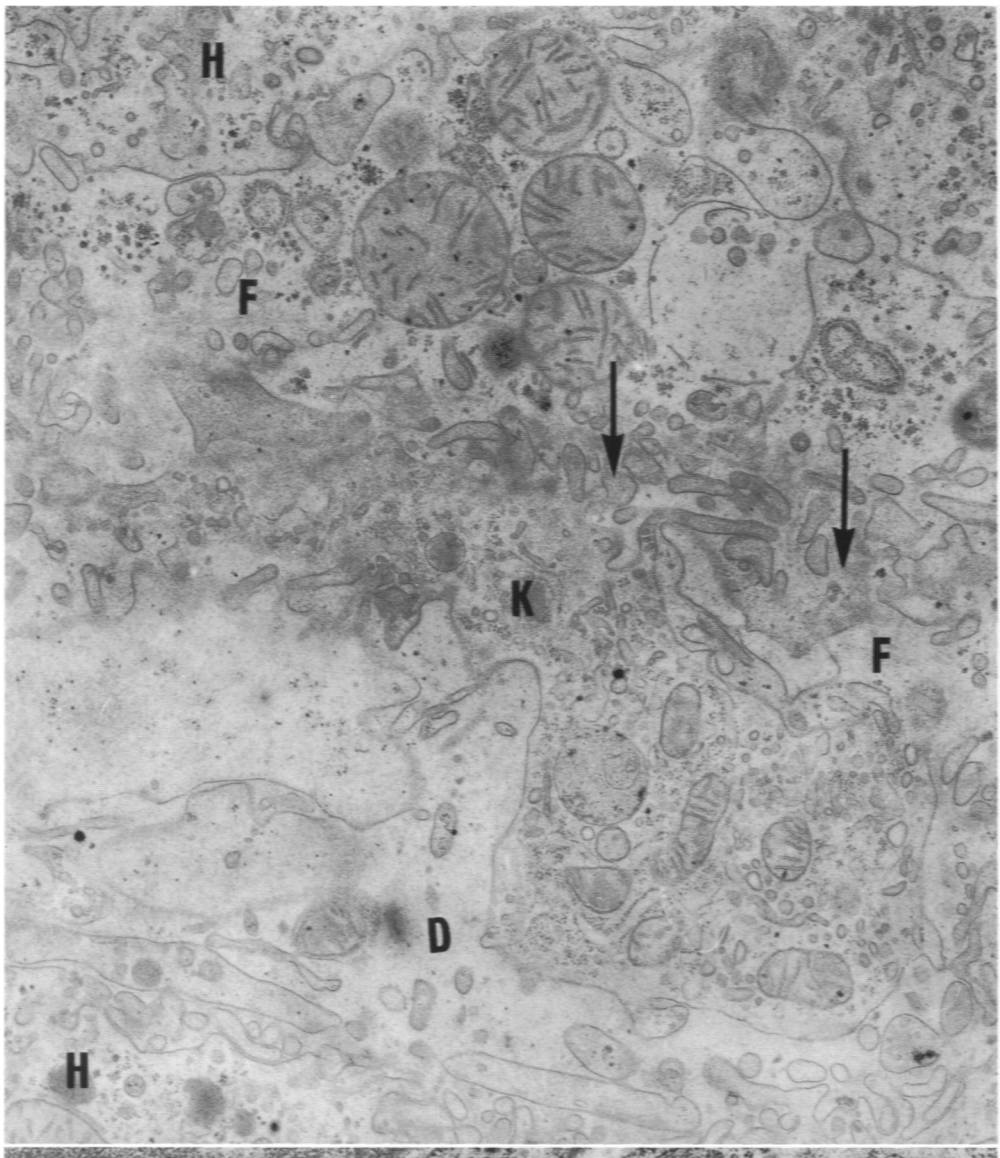

9

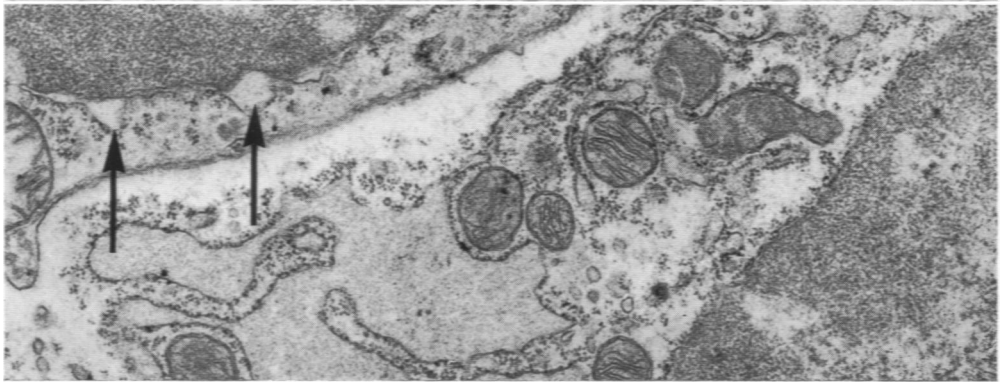

10

Fig. 11. At 24 hr. Acidophilic body (AB) in Kupffer cell. Fibrillar material also seen. × 22,300.

Fig. 12. At 1 hr. Focal separation between membranes of Kupffer cell nucleus (arrows) with apparent damage to outer membrane (barbed arrows). × 19,700.

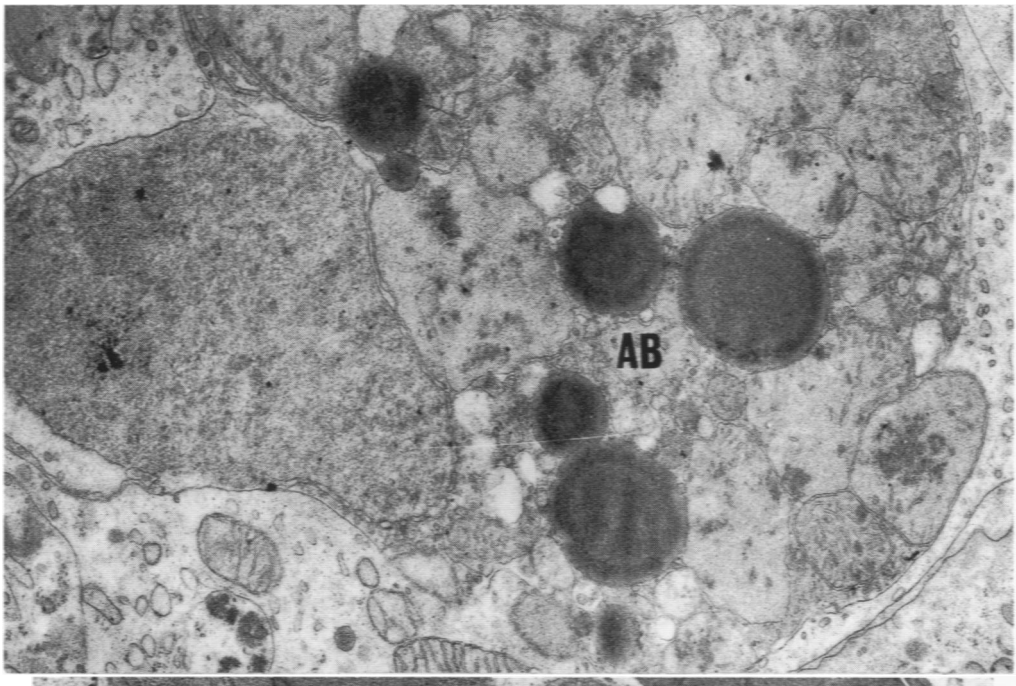

11

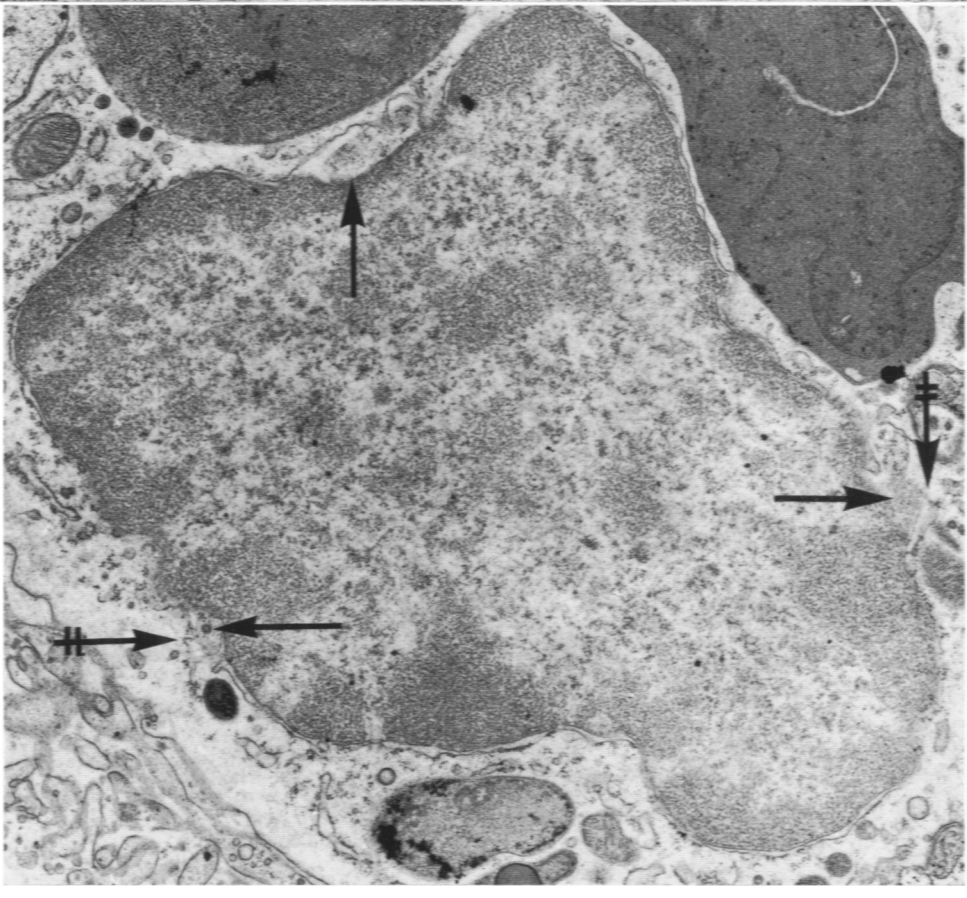

12

Fig. 13. At one-half hour. Vacuoles (V), some empty and others containing finely granular material, and dense bodies (L) in Kupffer cells. Edge of hepatocyte shown. × 20,000.

Fig. 14. 4 hr. Marked vacuolation of dense bodies (arrows) in region of hepatocytic nucleus. Uranyl acetate. × 9100.

Fig. 15. At 1 hr. Foci of necrosis (arrows) and dense body (L) in Kupffer cell. × 13,900.

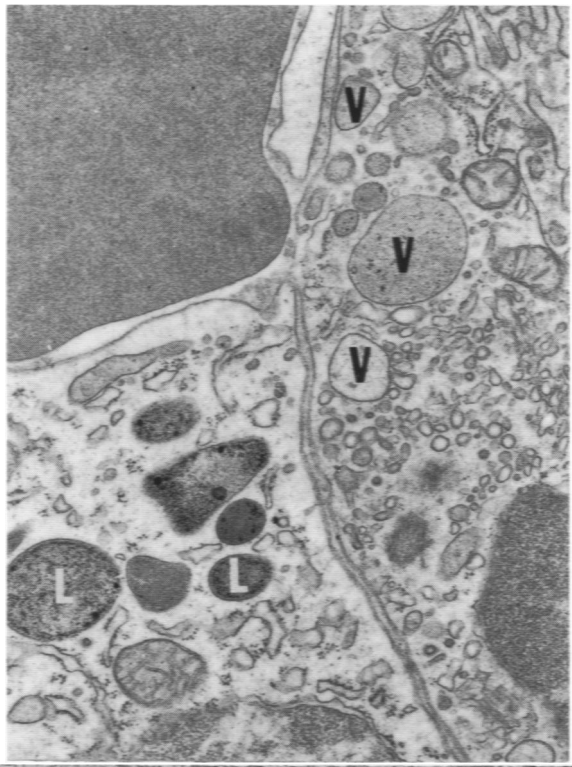

13

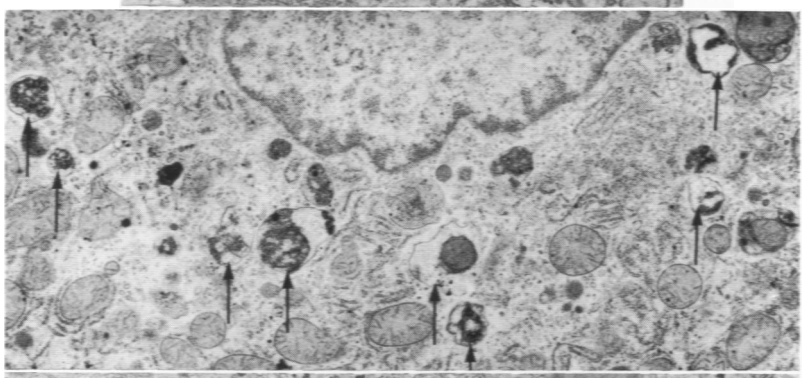

14

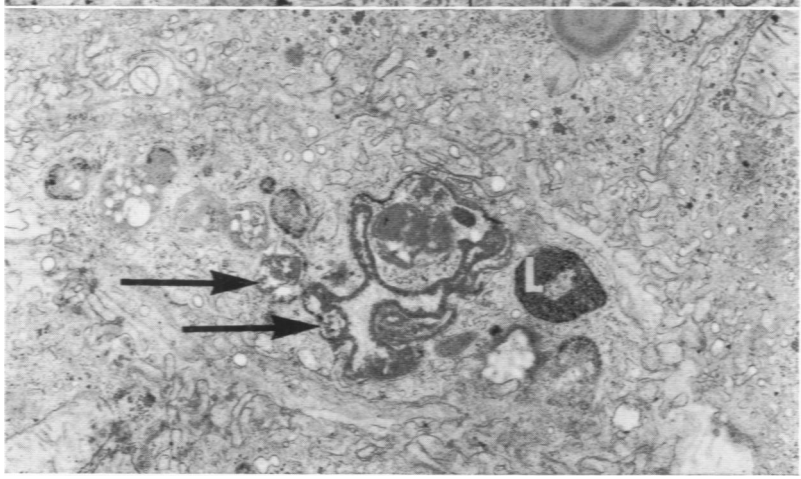

15

16

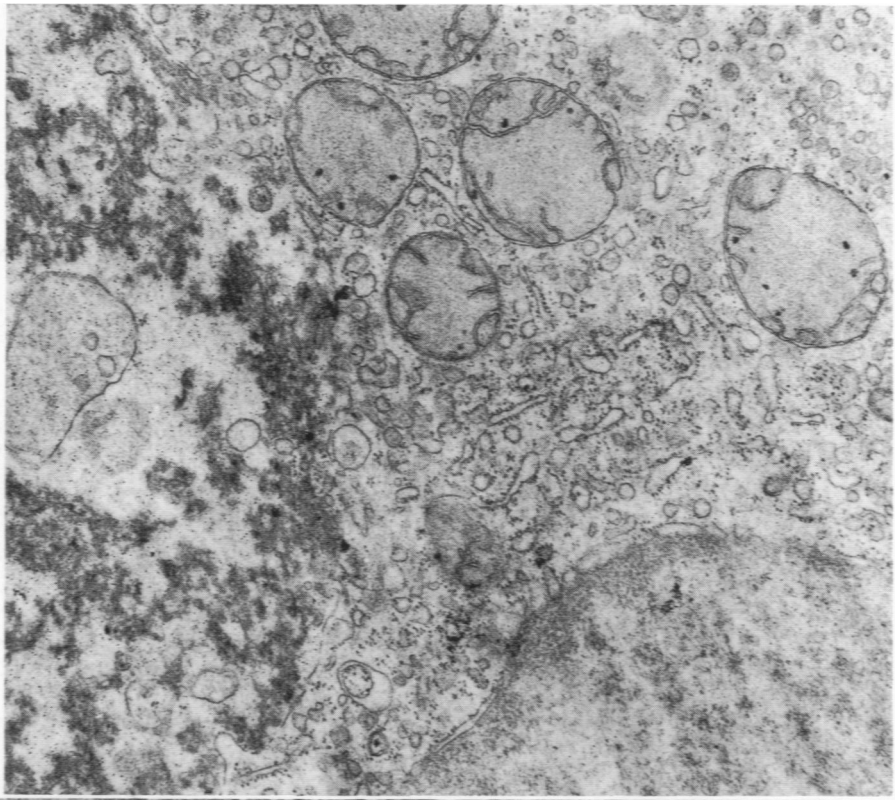

17

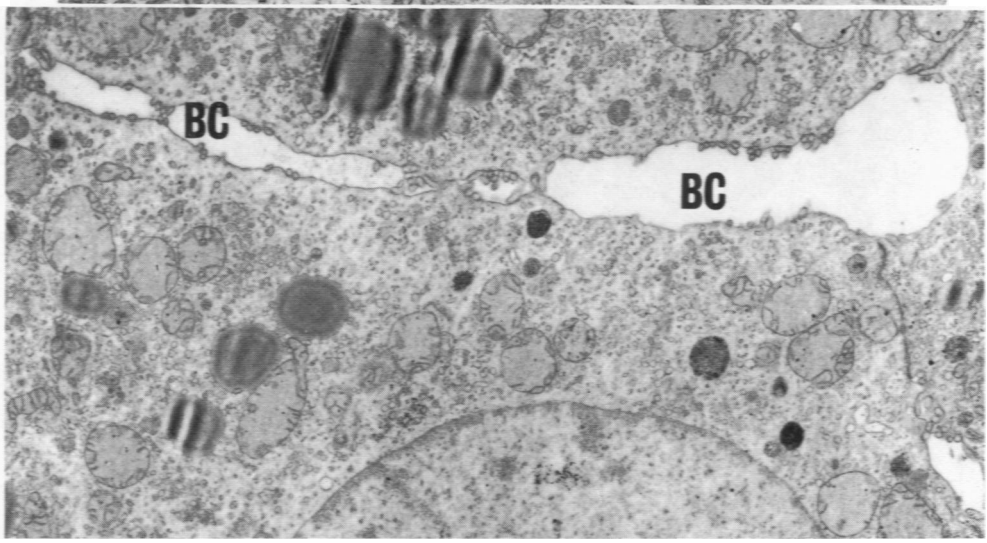

Fig. 16. At 24 hr. Focus of necrosis in hepatocyte at left half of picture. Note swollen mitochondria with curled cristae. × 30,500. **Fig. 17.** At 24 hr. Dilatation of bile canaliculi (BC) and loss of microvilli. Note also swelling of mitochondria with peripheral looping of cristae. × 10,200.